

Successful Stabilization of the Elusive Species {FeNO}⁸ in a Heme Model

Juan Pellegrino, Sara E. Bari, Damián E. Bikiel, and Fabio Doctorovich*

Departamento de Química Inorgánica, Analítica, y Química Física, Facultad de Ciencias Exactas y Naturales, Universidad de Buenos Aires, INQUIMAE-CONICET, Ciudad Universitaria, Pab. 2, C1428EHA Buenos Aires, Argentina

Received June 19, 2009; E-mail: doctorovich@qi.fcen.uba.ar

Abstract: Nitroxyl (HNO/NO⁻) heme-adducts have been postulated as intermediates in a variety of catalytic processes carried out by different metalloenzymes. Hence, there is growing interest in obtaining and characterizing heme model nitroxyl complexes. The one-electron chemical reduction of the {FeNO}⁷ nitrosyl derivative of Fe^{III}(TFPPBr₈)Cl, Fe^{II}(TFPPBr₈)NO (**1**) (TFPPBr₈ = 2,3,7,8,12,13,17,18-octabromo-5,10,15,20-[Tetrakis-(pentafluorophenyl)]porphyrin) with cobaltocene yields the significantly stable {FeNO}⁸ complex, [Co(C₅H₅)₂]⁺[Fe(TFPPBr₈)NO]⁻ (**2**). Complex **2** was isolated and characterized by UV-vis, FTIR, ¹H and ¹⁵N NMR spectroscopies. In addition, DFT calculations were performed to get more insight into the structure of **2**. According to the spectroscopic and DFT results, we can state unequivocally that the surprisingly stable complex **2** is the elusive {FeNO}⁸ species. Both experimental and computational data allow to assign the electronic structure of **2** as intermediate between Fe^{II}NO⁻ and Fe^INO, which is contrasted with the predominant Fe^{II}NO⁻ character of known *nonheme* {FeNO}⁸ complexes. The enhanced stability achieved for a heme model {FeNO}⁸ is expected to allow further studies related to the reactivity of this elusive species.

1. Introduction

The physiological importance of nitric oxide, NO, was accepted around two decades ago, and since then, a growing interest in the chemistry of heme-nitrosyls has started, as both the formation and activity of NO *in vivo* are mediated by heme proteins.¹ There has also been considerable interest over the past decade in the one-electron-reduced form of nitric oxide, nitroxyl (NO⁻ or HNO), because of the growing evidence for an independent biological significance of free nitroxyl itself.² This species might be created *in vivo* by nitric oxide synthase in the absence of its reduced bipterin cofactor.³ In addition, nitroxyl (HNO/NO⁻) heme-model complexes ({FeNO}⁸, according to the Enemark-Feltham notation) have received special attention due to the intermediacy of nitroxyl-heme adducts in a variety of catalytic processes related to the biogeochemical cycle of nitrogen.^{4,5} A better understanding of the structure and reactivity of these complexes is desirable and could help to elucidate mechanistic issues. While there are several examples of nitroxyl complexes with second- or third-row transition metals in the literature,⁶ only a few iron-nitroxyl complexes have been reported so far.

The complex Fe(NO)(cyclam-ac) was obtained by one-electron reduction of the {FeNO}⁷ complex in CH₃CN solution, giving a very air sensitive product in ~40% yield, and complete spectroscopic characterization was presented.⁷ Spectroscopic evidence for a six-coordinate deprotonated nitroxyl complex was further supported by density functional theory (DFT) calculations: the electronic structure of the complex was described as a low spin Fe^{II}(NO⁻). More recently, another non-heme {FeNO}⁸ complex was spectroscopically characterized in aqueous solution, after the two-electron reduction of the nitroprusside anion, [Fe(CN)₅(NO)]²⁻; this complex allowed the first pK_a determination of bound HNO, by ¹H NMR.⁸ While the protonated complex, [Fe(CN)₅(HNO)]³⁻ is stable in oxygen-free solutions, its conjugate base, [Fe(CN)₅(NO)]⁴⁻, decomposed to [Fe(CN)₅(NO)]²⁻ with a half-life of about 50 min.

The pioneering reports by Kadish et al. on the spectroelectrochemical reduction of Fe(TPP)NO and Fe(OEP)NO (TPP = 5,10,15,20-[Tetrakis-(phenyl)]porphyrin, OEP = 2,3,7,8,12,13,17,18-

- (1) Thomas, D. D.; Miranda, K. M.; Colton, C. A.; Citrin, D.; Espey, M. G.; Wink, D. A. *Antioxid. Redox Signaling* **2003**, *5*, 307–317.
- (2) (a) Stamler, J. S.; Singel, D. J.; Loscalzo, J. *Science* **1992**, *258*, 1898–1902. (b) Hughes, M. N. *Biochim. Biophys. Acta* **1999**, *1411*, 263–272.
- (3) Rusche, K. M.; Spiering, M. M.; Marletta, M. A. *Biochemistry* **1998**, *37*, 15503–15512.
- (4) {FeNO}ⁿ is the generalized description of the metal-NO bonding, where *n* is the sum of the metal d-electrons and the nitrosyl π* electrons. Enemark, J. H.; Feltham, R. D. *Coord. Chem. Rev.* **1974**, *13*, 339–406.

- (5) (a) Averill, B. A. *Chem. Rev.* **1996**, *96*, 2951–2964. (b) Garber, E. A. E.; Hollocher, T. C. *J. Biol. Chem.* **1982**, *257*, 4705–4708. (c) Dermastia, M.; Turk, T.; Hollocher, T. C. *J. Biol. Chem.* **1991**, *266*, 10899–10905. (d) Zumft, W. G. *Arch. Microbiol.* **1993**, *160*, 253–264. (e) Shiro, Y.; Fujii, M.; Iizuka, T.; Adachi, S. I.; Tsukamoto, K.; Nakahara, K.; Shoun, H. *J. Biol. Chem.* **1995**, *270*, 1617–1623. (f) Shiro, Y.; Fujii, M.; Isogai, Y.; Adachi, S. I.; Iizuka, T.; Obayashi, E.; Makino, R.; Nakahara, K.; Shoun, H. *Biochemistry* **1995**, *34*, 9052–9058. (g) Nakahara, K.; Tamimoto, T.; Hatauro, K.; Usuda, K.; Shoun, H. *J. Biol. Chem.* **1993**, *268*, 8350–8355.
- (6) Farmer, P. J.; Sulc, F. *J. Inorg. Biochem.* **2005**, *99*, 166–184.
- (7) Garcia Serres, R.; Grapperhaus, C. A.; Bothe, E.; Bill, E.; Weyhermuller, T.; Neese, F.; Wieghardt, K. *J. Am. Chem. Soc.* **2004**, *126*, 5138–5153.
- (8) Montenegro, A. C.; Amorebieta, V. T.; Slep, L. D.; Martín, D. F.; Roncaroli, F.; Murgida, D. H.; Bari, S. E.; Olabe, J. A. *Angew. Chem., Int. Ed.* **2009**, *48*, 4242–4245.

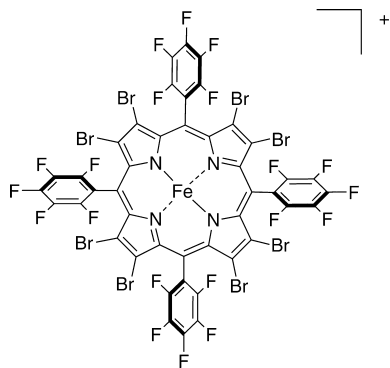


Figure 1. $[\text{Fe}^{\text{III}}(\text{TFPPBr}_8)]^+$.

octaethyl-5,10,15,20-[Tetrakis-(phenyl)]porphyrin) provided the first evidence of $\{\text{FeNO}\}^8$ porphyrinate complexes, in dichloromethane solutions.⁹ Following the track, Ryan et al. prepared $[\text{Fe}(\text{TPP})\text{NO}]^-$ in THF solution by both electrochemical and chemical reduction, and afforded further structural and reactivity insight.¹⁰ Albeit the anaerobic THF solution stabilized the $\{\text{FeNO}\}^8$ species, dichloromethane solutions gave back the $\{\text{FeNO}\}^7$ precursor, with a half-life of 30 min even at low temperatures. Further reduction allowed envisaging the presence of a $\{\text{FeNO}\}^9$ species by UV–vis, and exhaustive electrolysis in the presence of weak acids yielded hydroxylamine and ammonia as ultimate products.¹⁰

Stability of $\{\text{FeNO}\}^8$ complexes in aqueous solutions was first attained for a nitroxyl–myoglobin adduct, MbHNO,¹¹ and more recently in a series of $\text{Fe}^{\text{II}}(\text{globin})$ adducts by Farmer et al.¹² In these scenarios, the distal pocket residues provide extra stabilization to the bound HNO by hydrogen-bonding. The Mb(HNO) was fully characterized by NMR, Raman, and X-ray absorption spectroscopies.^{11,13} This complex is a six-coordinate HNO-adduct, and direct evidence of the H–N bond was obtained by ¹H NMR. Remarkably, the series of $\text{Fe}^{\text{II}}(\text{globin})\text{HNO}$ proteins represent the only $\{\text{FeNO}\}^8$ complexes obtained by direct trapping of free HNO from HNO-donor compounds.^{12,14}

Apparently, the main reason for the elusive nature of the NO[−] iron complexes previously reported is the high ease of oxidation to the stable $\{\text{FeNO}\}^7$ form. In order to enhance the stabilization of the heme model $\{\text{FeNO}\}^8$ moiety without the support of a protein environment, we focused on porphyrinates bearing electron-withdrawing substituents, aiming to tune the reduction potential of the heme-coordinated nitroxyl. In this work, we have synthesized $\text{Fe}^{\text{III}}(\text{TFPPBr}_8)\text{Cl}$ ($\text{TFPPBr}_8 = 2,3,7,8,12,13,17,18$ -octabromo-5,10,15,20-[Tetrakis-(pentafluorophenyl)]porphyrin, Figure 1) and the $\{\text{FeNO}\}^7$ nitrosyl iron complex $\text{Fe}^{\text{II}}(\text{TFPPBr}_8)\text{NO}$ (**1**) because it was hoped that upon one-electron reduction a fairly stable $\{\text{FeNO}\}^8$ complex would be

obtained. $\text{Fe}^{\text{III}}(\text{TFPPBr}_8)\text{Cl}$ assembles the ease of preparation and a highly positive shifted $\text{Fe}^{\text{III}}/\text{Fe}^{\text{II}}$ reduction potential (+600 mV from $\text{Fe}(\text{TPP})$).¹⁵ In this contribution, we describe the preparation, isolation, and spectroscopic characterization of a $\{\text{FeNO}\}^8$ complex, $[\text{Co}(\text{C}_5\text{H}_5)_2]^+[\text{Fe}(\text{TFPPBr}_8)\text{NO}]^-$ (**2**), obtained from reduction of **1** with the one-electron reductant cobaltocene. The electronic structure of the new complex was assessed by DFT calculations.

2. Experimental Section

2.1. Syntheses. 5,10,15,20-[Tetrakis-(pentafluorophenyl)]porphyrin (H_2TFPP) was purchased from Frontier Scientific and used as received. All other reagents were used as received, except $\text{Co}(\text{C}_5\text{H}_5)_2$ (Sigma-Aldrich) that was sublimed prior to use. All solvents were distilled and dried according to conventional procedures. The porphyrin ligand TFPPBr_8 and its iron(III) complex $\text{Fe}^{\text{III}}(\text{TFPPBr}_8)\text{Cl}$ were prepared according to slightly modified published procedures, starting from H_2TFPP .¹⁶

2.1.1. $\text{Fe}(\text{TFPPBr}_8)\text{NO}$ (1**).** This complex was prepared by reductive nitrosylation¹⁷ of $\text{Fe}^{\text{III}}(\text{TFPPBr}_8)\text{Cl}$. NO was bubbled through a solution of $\text{Fe}^{\text{III}}(\text{TFPPBr}_8)\text{Cl}$ (50 mg; 0.03 mmol) in degassed dichloromethane (10 mL) and methanol (5 mL) under a nitrogen atmosphere. NO was generated by dropwise addition of a solution of 500 mg of NaNO_2 in 8 mL of degassed water to a solution of 2.2 g of $\text{FeSO}_4 \cdot 7\text{H}_2\text{O}$ and 1 mL of H_2SO_4 in 15 mL of degassed water. NO was passed through a KOH column to remove higher oxides. The reaction was followed by UV–vis spectroscopy. The dilute solutions of $\text{Fe}^{\text{III}}(\text{TFPPBr}_8)\text{Cl}$ were brownish yellow, while those of **1** were greenish yellow. The reaction was easily followed by the shift of the Soret band from 402–442 to 430 nm. When maximum transformation was achieved, the solvent was removed *in vacuo*, and the product was purified by column chromatography in a drybox (stationary phase: acid alumina; mobile phase: anhydrous and degassed CH_2Cl_2); the first fraction was collected, the solvent was evaporated, and the solid residue was dried under vacuum. Yield: 0.030 g (60%). Anal. Calcd. for $\text{C}_{44}\text{N}_5\text{OFeBr}_8\text{F}_{20}$: C, 31.28; H, 0; N, 4.15. Found: C, 31.2; H, not detected; N, 4.3. UV–vis [CH_2Cl_2]: λ_{max} ($\epsilon/10^4$) = 430 nm (10.6), 580 nm (1.37). IR (cm^{-1}) (KBr pellet): ν_{NO} = 1726, isotope shift for the ¹⁵N(O)-labeled compound: -31 cm^{-1} .

2.1.2. $[\text{Co}(\text{Cp})_2]^+[\text{Fe}(\text{TFPPBr}_8)\text{NO}]^-$ (2**).** $\text{Co}(\text{Cp})_2$ was sublimed by heating at no more than 60 °C, under vacuum (0.1 mmHg), and kept and manipulated in a drybox. In a typical experiment, a solution of $\text{Co}(\text{Cp})_2$ of known concentration was achieved by dissolving 10 mg of the freshly sublimed reagent in anhydrous CH_2Cl_2 to a final volume of 1 mL. In a drybox, one equivalent of the dissolved $\text{Co}(\text{Cp})_2$ was added (approximately 100 μL) to a solution of 8 mg of **1** in 100 μL of anhydrous CH_2Cl_2 . The product, which precipitated after the addition of 3 mL of cold hexane, was separated from the solution by centrifugation, and the solid was dried under vacuum. Isolated yield: 90%. Anal. Calcd for $\text{C}_{54}\text{H}_{10}\text{Br}_8\text{F}_{20}\text{N}_5\text{OFeCo}$: C, 34.52; N, 3.73; H, 0.54. Found: C, 34.6; N, 3.6; H, 0.7. UV–vis [CH_2Cl_2]: λ_{max} ($\epsilon/10^4$) = 430 nm (8.14), 580 nm (1.65). IR (cm^{-1}) (solid film or CH_2Cl_2 solution): ν_{NO} = 1550 (sh). ¹H NMR (CD_2Cl_2): 4.94 (br s, 10H, $[\text{CoC}_{10}\text{H}_{10}]^+$). ¹⁵N NMR (CD_2Cl_2): 790 (s, br) (vs CH_3NO_2).

2.1.3. Synthesis of ¹⁵N(O)-Labeled **1 and **2**.** $\text{Fe}(\text{TFPPBr}_8)^{15}\text{NO}$ was prepared as described above, using ¹⁵NO prepared from $\text{Na}^{15}\text{NO}_2$; $[\text{Co}(\text{Cp})_2]^+[\text{Fe}(\text{TFPPBr}_8)^{15}\text{NO}]^-$ was prepared in a man-

- (9) (a) Lancon, D.; Kadish, K. M. *J. Am. Chem. Soc.* **1983**, *105*, 5610–5617. (b) Olson, L.; Schaefer, D.; Lancon, D.; Kadish, K. M. *J. Am. Chem. Soc.* **1982**, *104*, 2042–2044.
 (10) Choi, I. K.; Liu, Y.; Feng, D.; Paeng, K. J.; Ryan, M. D. *Inorg. Chem.* **1991**, *30*, 1832–1839.
 (11) Lin, R.; Farmer, P. J. *J. Am. Chem. Soc.* **2000**, *122*, 2393–2394.
 (12) Kumar, M. R.; Pervitsky, D.; Chen, L.; Poulos, T.; Kundu, S.; Hargrove, M. S.; Rivera, E. J.; Diaz, A.; Colón, J. L.; Farmer, P. J. *Biochemistry* **2009**, *48*, 5018–5025.
 (13) Immoos, C. E.; Sulc, F.; Farmer, P. J.; Czarnecki, K.; Bocian, D. F.; Levina, A.; Aitken, J. B.; Armstrong, R. S.; Lay, P. A. *J. Am. Chem. Soc.* **2005**, *127*, 814–815.
 (14) Sulc, F.; Immoos, C. E.; Pervitsky, D.; Farmer, P. J. *J. Am. Chem. Soc.* **2005**, *126*, 1096–1101.

- (15) Grinstaff, M. W.; Hill, M. G.; Birnbaum, E. R.; Schaefer, W. P.; Labinger, J. A.; Gray, H. B. *Inorg. Chem.* **1995**, *34*, 4896–4902.
 (16) (a) Birnbaum, E. R.; Hodge, J. A.; Grinstaff, M. W.; Schaefer, W. P.; Henling, L.; Labinger, J. A.; Bercaw, J. E.; Gray, H. B. *Inorg. Chem.* **1995**, *34*, 3625–3632. (b) Adler, A. D.; Longo, F. R.; Kampas, F.; Kim, J. J. *Inorg. Nucl. Chem.* **1970**, *32*, 2443–2445.
 (17) Wayland, B. B.; Olson, L. W. *J. Am. Chem. Soc.* **1974**, *96*, 6037–6041.

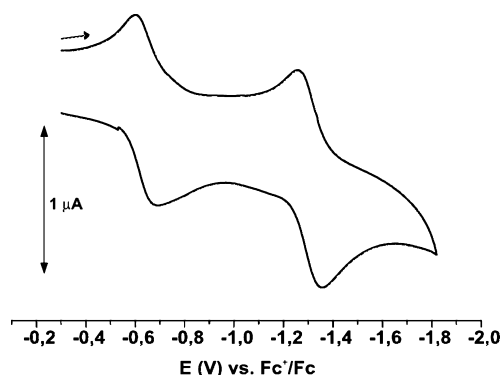


Figure 2. Cyclic voltammetry of **1** in CH₂Cl₂ (reduction waves).

ner analogous to that for the natural abundance compound, starting from Fe(TFPPBr₈)¹⁵NO.

2.2. Physical Measurements. Cyclic voltammetry was carried out at 100 mV/s scan rate in dry and deoxygenated CH₂Cl₂/0.1 mol dm⁻³ Bu₄NPF₆ using a three-electrode configuration (glassy carbon or Pt working electrode, Pt counter electrode, Ag wire pseudoreference electrode) and a PAR 273 or TEQ 03 potentiostat. The ferrocenium/ferrocene (Fc⁺⁰) couple served as internal reference. The solutions were prepared under Ar or N₂, in a drybox or using a vacuum line, at concentrations of approximately 1 mM.

UV–vis spectra were acquired on a Hewlett-Packard HP8453 diode array spectrometer with 1 cm path length cells, under Ar or N₂, preparing the solutions in a drybox or by using a vacuum line, at concentrations of approximately 10⁻² mM.

FTIR spectra were acquired with a Nicolet Avatar FTIR spectrophotometer. Solution spectra were obtained using a demountable cell, with NaCl or CaF₂ windows, under Ar or N₂, preparing the solutions in a drybox or by using a vacuum line, typical concentration 10 mM. Solid-state spectra were obtained as KBr pellets for non-air-sensitive compounds. Solid FTIR spectra of **2** were obtained from a film prepared by evaporation of a concentrated CH₂Cl₂ solution on a NaCl window, in a drybox. The closed cell was taken out of the box and immediately placed in the spectrometer.

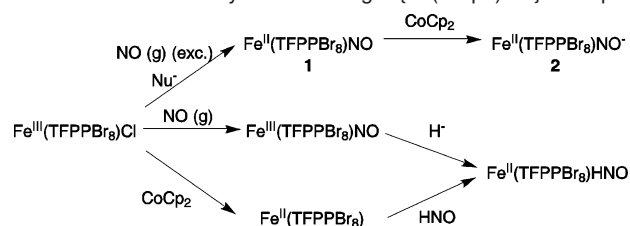
The ¹H and ¹⁵N NMR spectra were acquired on a Bruker 500 MHz instrument, with dry and deoxygenated CH₂Cl₂ solutions of the reduced complex (**2**), containing 25% CD₂Cl₂, at room temperature. The CH₂Cl₂ signal was suppressed. The solutions were prepared in a drybox, under N₂, at concentrations of approximately 30 mM.

2.3. Computational Methodology. All calculations were carried out with the program package Gaussian 03.¹⁸ The structures of all molecules were fully geometry optimized at the DFT level, using the PBE exchange–correlation functional. LANL2DZ basis set and pseudopotential were used for the Fe atom. For the remaining atoms (H, N, O, C, F, and Br) the 6-31G** basis set was used. Molecular orbital coefficients were parsed and viewed using QMForge to calculate molecular orbital contributions from groups of atoms.¹⁹ Charges were calculated by performing a natural population analysis (NPA).

3. Results and Discussion

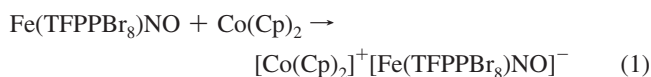
3.1. Synthetic Strategies for the Preparation of the {FeNO}⁸ Porphyrin Complex. The synthetic scheme for the obtention of **2** comprises two steps: (1) the preparation of the {FeNO}⁷ complex, Fe^{II}(TFPPBr₈)NO (**1**), by reductive nitrosy-

Scheme 1. Possible Ways of Obtaining a {Fe(Porph)NO}⁸ Complex



lation of Fe^{III}(TFPPBr₈)Cl and (2) the one-electron reduction of **1**. Cyclic voltammetry of **1** in CH₂Cl₂ (Figure 2) shows two, well reversible reduction waves at *E*_{1/2} -0.65 V and -1.33 V vs Fc⁺/Fc, respectively, shifted +770 and +940 mV from the corresponding values of Fe^{II}(TPP)NO.^{9,10}

Accordingly, the bis(cyclopentadienyl)cobalt(II), Co(Cp)₂ (*E* = -1.30 V vs Fc⁺/Fc),²⁰ was chosen for the one-electron reduction of **1**. A new complex (**2**) was obtained by stoichiometric addition of Co(Cp)₂ to **1**, eq 1, after precipitation with hexane. Elemental analysis revealed the presence of the cobaltocenium cation, [Co(Cp)₂]⁺ as the counterion and is consistent with the structure proposed in eq 1.



The complex redox chemistry of NO leads to a variety of methods yielding {MNO}⁸ complexes.⁶ According to what is already known on nitrosyl metalloporphyrins, one can envision three different ways of obtaining a Fe(Porph)(NO⁻/HNO) complex (Scheme 1), the first path being our choice for the preparation of **2**.

The second path depicted in Scheme 1 comprises the first step of formation of an {FeNO}⁶ complex (Fe^{III}NO) and then a nucleophilic hydride attack on the {FeNO}⁶, following the approach of Richter Addo et al. for the preparation of Ru(TTP)(HNO)(1-MeIm)] (TTP = 5,10,15,20-[Tetrakis-(tolyl)]porphyrin, 1-MeIm = 1-methylimidazole).²¹ This strategy is restricted by the instability of {FeNO}⁶ precursors (the reductive nitrosylation, that would give the {FeNO}⁷ complex, is difficult to avoid), in contrast to the highly stable {RuNO}⁶ analogues.^{22,23} Another option would be trapping free HNO by a pentacoordinate metal complex, as illustrated in the third path in Scheme 1. This reaction has been reported for a survey on Fe^{II}(globins).^{12,14} In organic media, this approach could be applied to the direct reaction of stable Fe^{II} porphyrinate complexes toward adequate nitroxyl donors, for example, benzenesulfohydroxamic acid. The stability of the iron II state toward oxidation can be attained by the insertion of withdrawing substituents in the porphyrin periphery,¹⁵ as mentioned above. In this procedure, the expected reactivity of the emerging {FeNO}⁸ complex toward excess HNO or the HNO donor could considerably decrease the yield of the desired complex.^{6,12} Preliminary attempts on the reaction of Fe^{II}(TFPPBr₈) with toluenesulfohydroxamic acid as the HNO donor in organic media did not reveal the presence of {FeNO}⁸ as judged by UV–vis (data not shown). Hence, the first procedure in Scheme 1, consisting in the one-electron reduction of an {MNO}⁷ complex, seems to be the best choice to obtain

(20) Gennett, T.; Milner, D. F.; Weaver, M. J. *J. Phys. Chem.* **1985**, *89*, 2787–2794.

(21) Lee, J.; Richter-Addo, G. B. *J. Inorg. Biochem.* **2004**, *98*, 1247–1250.

(22) Praneeth, V. K. K.; Paulat, F.; Berto, T. C.; George, S. D.; Näther, C.; Sulok, C. D.; Lehnert, N. *J. Am. Chem. Soc.* **2008**, *130*, 15288–15303.

(23) Wyllie, G. R. A.; Scheidt, W. R. *Chem. Rev.* **2002**, *102*, 1067–1089.

(18) Frisch, M. J., et al. *Gaussian 03*, Revision C.02; Gaussian, Inc.: Wallingford CT, 2004.

(19) Tenderholt, A. L. *QMForge*, Version 2.1; <http://qmforge.sourceforge.net>, 2007.

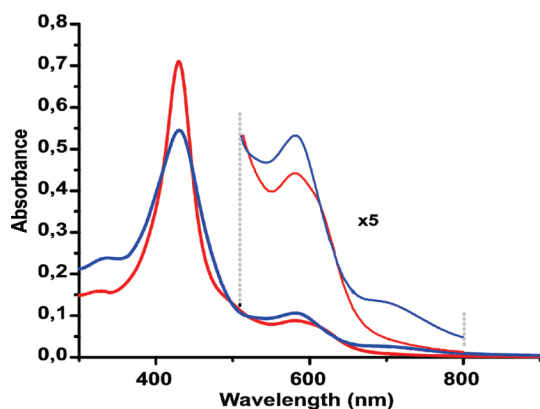


Figure 3. UV-vis spectra of **1** (red) and **2** (blue) in CH_2Cl_2 .

the $\{\text{Fe}(\text{Porph})\text{NO}\}^8$ complex, as the reaction scheme excludes the formation of $\{\text{FeNO}\}^6$ intermediates and the reaction media can be controlled by strict stoichiometric addition of reductant, thus avoiding undesired secondary reactions.

3.2. Spectroscopic Characterization of $[\text{Co}(\text{Cp})_2]^+[\text{Fe}(\text{TFPPBr}_8)\text{NO}]^-$ (2**).** The ^1H NMR spectra of **2** (Supporting Information) shows a peak assignable to cobaltocenium and no other relevant signal, suggesting a five-coordinate and deprotonated $\{\text{FeNO}\}^8$ complex, as expected for the aprotic, noncoordinating reaction media used to carry out the preparation.

The electronic absorbance bands of **2** appear at wavelengths similar to those of **1**, but with lower intensity of the Soret absorbance and subtle changes in the Q-bands (Figure 3). These features of the UV-vis spectra of heme $\{\text{FeNO}\}^{7/8}$ complexes were previously reported for MbNO and Mb(HNO) and for $\text{Fe}^{\text{II}}(\text{TPP})\text{NO}$ and $[\text{Fe}^{\text{II}}(\text{TPP})\text{NO}]^-$.^{10,11} The minor changes in the Soret band in the UV-vis spectrum upon reduction firmly suggest a non-porphyrin-centered reduction.

In the solution FTIR spectrum of **2**, ν_{NO} (1715 cm^{-1}) disappears completely after the addition of one equivalent of $\text{Co}(\text{Cp})_2$, with apparently no new emerging signals (Figure 4, left). FTIR ν_{NO} values for the $\{\text{MNO}\}^n$ moieties are known to be very sensitive to n , decreasing with n from $6 \rightarrow 8$ (NO-centered reduction).²⁴ Specifically, ν_{NO} in the $\{\text{FeNO}\}^8$ complex TPPFeNO^- was reported at 1496 cm^{-1} ,¹⁰ and previous calculations suggest values of $\sim 1500\text{ cm}^{-1}$.²⁵ Accordingly, the band corresponding to ν_{NO} in **2** is expectedly masked by the intense bands at $1450\text{--}1550\text{ cm}^{-1}$, and only part of a broad signal around 1550 cm^{-1} is exposed. The presence of the withdrawing groups shifts the band position at higher frequency, as a consequence of the decrease of π back-bonding from the iron center to the NO^- ligand (*vide infra*). Signal width could be attributed to the contribution of rotational conformers of the ligand. In the enriched $\text{Fe}(\text{TFPPBr}_8)^{15}\text{NO}$, the exposed tail of the signal is now totally masked, as a result of the expected red isotopic shift. Noteworthy, **1** can be completely regenerated from **2** after the addition of one equivalent of the one-electron oxidant ferrocenium hexafluorophosphate (see Supporting Information). The shift from 1716 cm^{-1} to 1550 cm^{-1} upon the addition of a one equivalent reductant is indicative of a $\{\text{FeNO}\}^7$ to $\{\text{FeNO}\}^8$ conversion. Moreover, in the solid-state FTIR spectra of isolated **2** there is no signal corresponding to the $\{\text{FeNO}\}^7$ precursor,

and a defined shoulder around 1550 cm^{-1} is present. Remarkably, in the solid-state spectra measured during the following minutes, the shoulder decreases progressively until it disappears, while the 1715 cm^{-1} band is partially recovered. The difference spectrum shows a well-defined band at 1547 cm^{-1} (Figure 4, right, inset). These changes must be the result of the reaction of solid **2** with the oxygen present in air, which cannot be strictly avoided. The only partial recovery of the band assigned to **1** suggests the formation of other oxidation products apart from **1**. The same result is obtained by the oxidation of **2** under air, in CH_2Cl_2 solution as judged by UV-vis and FTIR (data not shown).

Conclusive evidence for the identity of complex **2** is given by the ^{15}N NMR spectrum of the ^{15}N -labeled compound $[\text{Co}(\text{Cp})_2]^+[\text{Fe}(\text{TFPPBr}_8)^{15}\text{NO}]^-$ (Figure 5), showing only one signal at $+790\text{ ppm}$ vs $\text{CH}_3^{15}\text{NO}_2$, a value in the upper limit of previously characterized bent nitrosyl complexes.²⁶ The dramatic dependence of the nitrogen shift with the MNO angle in metal nitrosyls has been reviewed,²⁷ with deshieldings of up to 800 ppm for strongly bent nitrosyls $\{\text{MNO}\}^8$ compared with linear nitrosyls $\{\text{MNO}\}^6$. In addition, the observation of the ^{15}N NMR signal for $^{15}\text{N}(\text{NO})$ enriched **2** shows that the species is diamagnetic.

3.3. Density Functional Calculations. Density functional theory calculations *in vacuo* were performed to give more insight into the electronic structure of **2**. The anionic portion of **2** (it will simply be referred as **2** in the following) was calculated both in the singlet and triplet state, with the singlet state being more stable by 15 kcal/mol , which is consistent with the observation of the ^{15}N NMR signal. The porphyrin ring is quite distorted and nonplanar due to the presence of the bulk bromine substituents (Figure 6).

3.3.1. Bonding Parameters of **1 and **2**.** Table 1 shows the relevant bond distances and angles for the calculated structures of **1** and **2**, compared with experimental and calculated data for other $\{\text{FeNO}\}^{7/8}$ complexes.^{13,28–30}

As commonly observed in $\{\text{FeNO}\}^7$ model hemes the FeNO unit in **1** is bent with an FeNO angle of $\sim 144^\circ$. The Fe–NO distance of 1.71 \AA is in good agreement with the experimental findings. As can be seen in Table 1, experimental values for the N–O distance show considerable variation, probably due to the usual disorder in the $\{\text{MNO}\}^7$ unit. However, the calculated value of 1.18 \AA for the N–O distance in **1** is in good agreement with calculated values for other $\{\text{FeNO}\}^7$ systems. Upon reduction of **1** to the $\{\text{FeNO}\}^8$ form, **2**, the Fe–N bond lengthens considerably to 1.79 \AA , the FeNO angle decreases to $\sim 123^\circ$, and the N–O bond lengthens to 1.20 \AA , which is again in good agreement with previous calculations (we have not compared these data with experimental data because, to the best of our knowledge, there is no experimental structure for a deprotonated $\{\text{FeNO}\}^8$ system).

The bonding parameters for triplet **2** are remarkably different to the ones for singlet **2**, and in fact, they are similar to the ones for **1**. Our results, in agreement with previous calculations,²⁵ indicate that in the $\{\text{FeNO}\}^8$ triplet state the added electron fills a porphyrin orbital, and so it is better described as

(24) Sellmann, D.; Gottschalk-Gaudig, T.; Haussinger, D.; Heinemann, F. W.; Hess, B. A. *Chem.–Eur. J.* **2001**, *7*, 2099–2103.

(25) Lehnert, N.; Praneeth, V. K. K.; Paulat, F. *J. Comput. Chem.* **2006**, *27*, 1338–1351.

(26) Bultitude, J.; Larkworthy, L. F.; Mason, J.; Povey, D. C.; Sandell, B. *Inorg. Chem.* **1984**, *23*, 3629–3633.

(27) Mason, J.; Larkworthy, L. F.; Moore, E. A. *Chem. Rev.* **2002**, *102*, 913–934.

(28) Bohle, D. S.; Hung, C.-H. *J. Am. Chem. Soc.* **1995**, *117*, 9584–9585.

(29) Scheidt, W. R.; Frisse, M. E. *J. Am. Chem. Soc.* **1975**, *97*, 17–21.

(30) Einsle, O.; Messerschmidt, A.; Huber, R.; Kroneck, P. M. H.; Neese, F. *J. Am. Chem. Soc.* **2002**, *124*, 11737–11745.

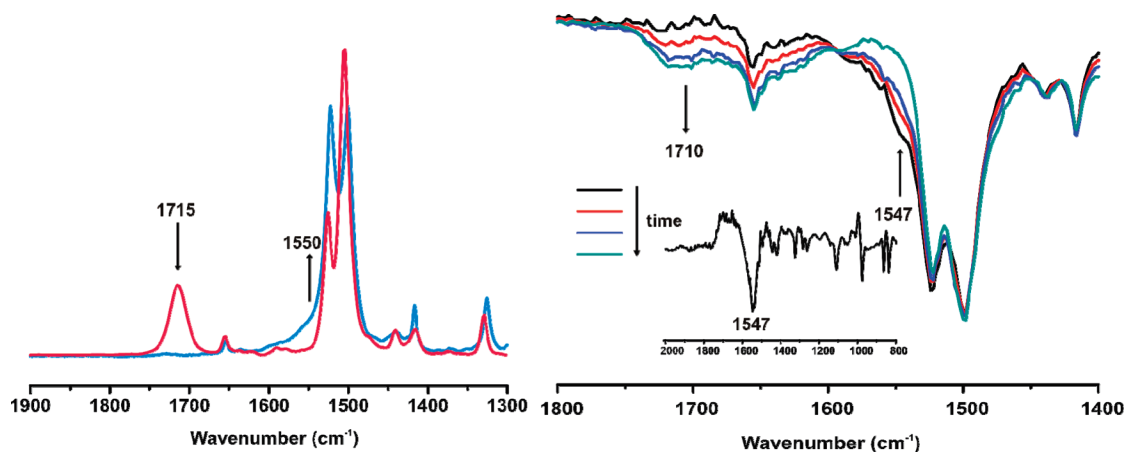


Figure 4. FTIR spectra of **1** (red) and **2** (blue) in CH₂Cl₂ (left) and solid film FTIR spectrum of **2** (right). Black: initial spectrum. Inset: difference spectrum of the initial and last spectra.

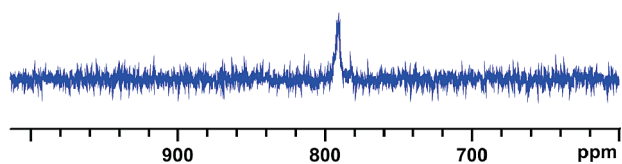


Figure 5. ¹⁵N NMR spectrum of [Co(Cp)₂]⁺[Fe(TFPPBr₈)¹⁵NO]⁻ in CH₂Cl₂.

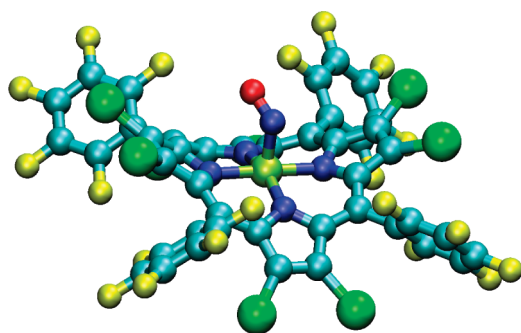


Figure 6. DFT calculated structure of **2**.

Table 1. Selected Bond Lengths (Å) and Angles (deg) for Calculated Structures of **1**, **2** and Related {FeNO}^{7/8} Complexes

	d(NO)	d(FeN)	∠FeNO	ref
1 ^b	1.182	1.711	144.4	this work
Fe(TPPBr ₈)NO ^a	1.42	1.75	146	28
Fe(TPP)NO ^a	1.122	1.717	149.2	29
Fe(Porphine)NO ^b	1.179	1.705	146	this work
2 singlet ^b	1.201	1.790	122.7	this work
2 triplet ^b	1.181	1.747	154.8	this work
Mb(HNO) ^a	1.24	1.82	131	13
Fe(Porphine)NO ^{-b}	1.211	1.778	123.1	this work
[Fe(Porphine)(NH ₃)(NO)] ^{-b}	1.21	1.79	126	30

^a Experimental values. ^b Calculated.

an iron(II) coordinated to a porphyrin radical and a NO neutral ligand (reduction centered in the porphyrin ring). Due to the presence of strong withdrawing groups, a porphyrin-centered reduction in **1** could have been expected. However, the ¹⁵N NMR result and the DFT calculations show clearly that the {FeNO}⁸ product **2** is definitely in its singlet state.

3.3.2. Bonding Description of Complex 2. In order to develop a bonding scheme between the iron and NO we will consider

Table 2. Percentage Contributions of Important Molecular Orbitals of **2** and [Fe(Porphine)NO]⁻ from Different Fragments

		Fe						
		porphyrin	NO	d _{z²}	d _{xz}	d _{yz}	d _{xy}	d _{x²-y²}
Fe(Porph)NO ⁻	HOMO	21	25	23	29	0	0	0
	HOMO-1	7	1	0	2	0	0	90
	HOMO-2	14	31	11	38	0	0	4
	LUMO+2	9	65	0	0	25	0	0
2	HOMO	28	27	22	9	13	0	0
	HOMO-1	24	23	9	16	17	10	0
	HOMO-2	12	3	1	0	4	78	1
	LUMO+3	15	64	0	14	6	0	0

the metal center to be in the +2 oxidation state (low spin) and the nitric oxide as an NO⁻ in its singlet state. For a five-coordinate nitrosyl iron complex, the electron configuration of the metal would be [d_{yz}, d_{yz}, d_{xy}]^{6, 31} and the HOMO and the LUMO for singlet NO⁻ are π_h* and π_v* respectively (h = horizontal, v = vertical; this notation makes sense when considering the interaction of these orbitals in the whole complex, the horizontal orbital being located in the Fe–N–O plane whereas the vertical one is perpendicular to that plane). Table 2 shows the composition of important molecular orbitals of **2** compared with those of [Fe(Porphine)NO]⁻ in order to examine the influence of the electron withdrawing groups in the electronic structure.

The HOMO and HOMO-1 of complex **2** (Figure 7) are Fe–NO bonding and reflect a very important σ bond through donation of electron density from the doubly occupied π_h* orbital of NO to the empty d_{z²} orbital of iron. The equivalent molecular orbitals that reveal this σ bond in [Fe(Porphine)NO]⁻ are the HOMO and the HOMO-2 of this complex (Figure 7). The main difference is that these orbitals have less contribution from porphyrin orbitals, and a bit more from occupied orbitals of NO or Fe in [Fe(Porph)NO]⁻ compared to **2**. So, as expected, the effect of the withdrawing groups is to move some electron density from occupied orbitals of iron and NO to porphyrin orbitals. On the other hand, the σ interaction between NO and iron is slightly reduced in **2** because of the competition for electron density of the deficient porphyrin ring.

Additional contribution to the Fe–N(O) bond in **2** is given by π back-bonding interaction between the empty π_v* orbital

(31) Scheidt, W. R.; Reed, C. A. *Chem. Rev.* **1981**, *81*, 543–555.

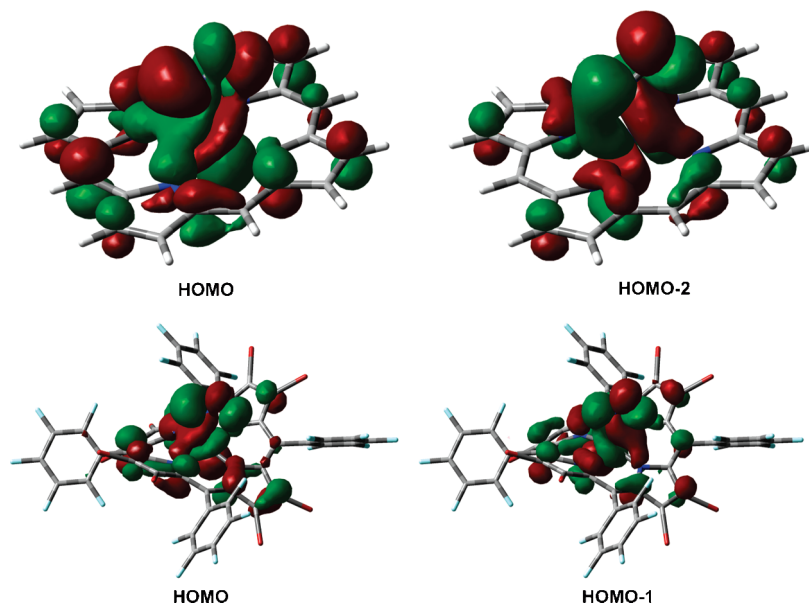


Figure 7. Frontier molecular orbitals of $[\text{Fe}(\text{Porphine})\text{NO}]^-$ (top) and **2** (bottom) showing the σ interaction between NO and iron.

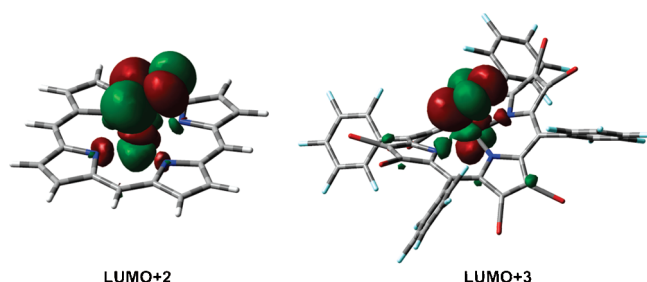


Figure 8. Frontier molecular orbitals of $[\text{Fe}(\text{Porphine})\text{NO}]^-$ (left) and **2** (right) showing the π interaction between NO and iron.

of NO and the doubly occupied d_{xz} and d_{yz} orbitals of iron, which is reflected in the LUMO+3 (Figure 8); this orbital corresponds to the antibonding combination. In $[\text{Fe}(\text{Porph})(\text{NO})]^-$ this interaction is evidenced in LUMO+2 (Figure 8). Again, the competition of the porphyrin ring is present, resulting in slightly reduced π back-donation in **2** as one can see from the percentage contributions in Table 2. Moreover, in the LUMO+3 of **2**, the iron orbital is oriented toward two N pyrrolic atoms that allow interaction with a porphyrin orbital, whereas in $[\text{Fe}(\text{Porph})(\text{NO})]^-$ the d_{yz} orbital contributing to LUMO+2, is oriented between the N pyrrolic atoms so that no interaction with the porphyrin ring is possible. Additionally, the orientation of the NO ligand on each structure is different, which is related to the distinct symmetry of the complexes.

The slight effect of the withdrawing substituents on the Fe–NO bond is also reflected in the calculated Fe–N and N–O distances (Table 1). The Fe–N bond is a bit longer in **2**, a consequence of the reduced σ and π interactions, as previously discussed, while the N–O bond is a bit shorter, due to the reduced π back-donation.

These calculations suggest that the limiting description of **2** as an $\text{Fe}^{\text{II}}\text{NO}^-$ complex is not entirely correct and the actual electronic structure is intermediate between $\text{Fe}^{\text{II}}\text{NO}^-$ and $\text{Fe}^{\text{I}}\text{NO}$, in agreement with the calculations of Lehnert et al. on $[\text{Fe}(\text{Porph})(\text{MI})(\text{NO})]^-$ (MI = methylimidazole).²⁵ On the other hand, the electronic structure of the non-heme $\{\text{FeNO}\}^8$ complex $\text{Fe}(\text{NO})(\text{cyclam-ac})^-$ fits well with the limiting description of a low spin $\text{Fe}^{\text{II}}(\text{NO})^-$.⁷ As for the effect of the sixth ligand, our calculations on

Table 3. Selected Parameters for **2**, $[\text{Fe}(\text{Porphine})\text{NO}]^-$, and $\text{Fe}(\text{NO})(\text{cyclam-ac})^-$ That Reveal the Difference in Its Electronic Structures

	2	$[\text{Fe}(\text{Porphine})\text{NO}]^-$	$\text{Fe}(\text{NO})(\text{cyclam-ac})^-$ ⁷
$d(\text{NO})$ (pm)	120.1	121.1	126.1
$\Delta d(\text{NO})$ (pm) ^a	2.6	1.9	5.7
$\angle\text{FeNO}$ (deg)	122.7	123.1	122.4
$\Delta \angle\text{FeNO}$ (deg) ^a	-21.7	-19.3	-18.2
ν_{NO} (cm^{-1})	1547 ^b	1530 ^c	1271 ^d
$\Delta \nu_{\text{NO}}$ (cm^{-1}) ^a	-165	-159	-336
charge on NO	-0.134	-0.217	-0.672
Δ charge on NO ^a	-0.146	-0.207	-0.442
charge on Fe	0.552	0.556	0.882
Δ charge on Fe ^a	-0.103	-0.137	-0.123

^a Δ refers to the difference between the value of the $\{\text{FeNO}\}^8$ complex and the corresponding $\{\text{FeNO}\}^7$ precursor. ^b Experimental value, solid state. ^c Calculated, scaled factor = 0.961. ^d Experimental value, in CH_3CN .

Table 4. Calculated Natural Population (NPA) for **1**, **2**, $\text{Fe}(\text{TPP})\text{NO}$, and $[\text{Fe}(\text{TPP})\text{NO}]^-$

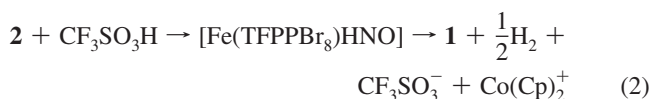
	FeTPPNO	$[\text{FeTPPNO}]^-$	1	2
Fe	0.69	0.56	0.66	0.55
NO	-0.02	-0.21	0.01	-0.13
Porph	-0.67	-1.35	-0.67	-1.42

$[\text{Fe}(\text{Porphine})\text{NO}]^-$ compared with the computational results on $[\text{Fe}(\text{Porph})(\text{MI})(\text{NO})]^-$ suggest similar electronic structures for the five- and six-coordinate $\{\text{FeNO}\}^8$ complexes, differently from what has been found in five- and six-coordinate heme $\{\text{FeNO}\}^7$ complexes.³² Table 3 shows selected parameters relevant to the FeNO moiety for **2**, $[\text{Fe}(\text{Porphine})\text{NO}]^-$, and $\text{Fe}(\text{NO})(\text{cyclam-ac})^-$ in order to determine the influence of different environments in the structure of $\{\text{FeNO}\}^8$. As can be seen, there is a much more considerable change in the electronic structure of the $\{\text{FeNO}\}^8$ moiety upon changing the porphyrin ring by a non-heme ligand than by the presence of the withdrawing groups in the porphyrin periphery, as expected. Although there is a mention of similarity

(32) (a) Praneeth, V. K. K.; Näther, C.; Peters, G.; Lehnert, N. *Inorg. Chem.* **2006**, *45*, 2795–2811. (b) Praneeth, V. K. K.; Neese, F.; Lehnert, N. *Inorg. Chem.* **2005**, *44*, 2570–2572.

between NO binding to heme and non-heme iron centers in the literature,⁷ our findings, in agreement with the calculations of Lehnert et al. on [Fe(Porph)(MI)(NO)]⁻, show that the electronic structures of heme and non-heme {FeNO}⁸ differ considerably. The results obtained for Fe(NO)(cyclam-ac) are consistent with a predominant Fe^{II}NO⁻ electronic structure,⁷ while for *heme* {FeNO}⁸ complexes an intermediate structure between Fe^{II}NO⁻ and Fe^INO seems to be more appropriate. Noteworthy, the FeNO angle is ~120° in all three {FeNO}⁸ complexes, suggesting that this parameter is not very sensitive to the distribution of electron density in the MNO moiety, as predicted by Enemark and Feltham,⁴ while N–O distance and ν_{NO} seem to be the most sensitive parameters.

3.4. Reactivity of 2. UV–vis and FTIR spectra of the reaction of **2** with one equivalent of triflic acid indicate that there is back-oxidation to **1**, probably with the intermediacy of an Fe^{II}(HNO) complex and the formation of H₂, as shown in eq 2. No reaction is observed when one equivalent of acetic acid is added to **2** (see Supporting Information).



This reactivity has been previously reported for [Fe(TP-P)NO]⁻ with phenol as the proton source.¹⁰ The participation of the withdrawing halogen substituents in the ligand reactivity is evaluated in Table 4, by performing a normal population analysis for the charges on complexes Fe(TPP)NO, [Fe(TP-P)NO]⁻, **1**, and **2**. The negative charge on the NO moiety for [Fe(TFPPBr₈)NO]⁻ is about half of that on [Fe(TPP)NO]⁻ (0.13 vs 0.21). This is consistent with the requirement of a much stronger acid to achieve reoxidation of **2** to **1**. Apart from Mb(HNO) and other globins, there is only one reported HNO–metalloporphyrin complex, [Ru(TTP)(HNO)(1-MeIm)].²¹ The difference in stabilities of these six-coordinate protonated {M(Porph)NO}⁸ compared to five-coordinate protonated **2** may be attributed to extra stabilization by distal amino acids in Mb(HNO) or by the ruthenium metal center in [Ru(TTP)(HNO)(1-MeIm)], though the trans ligand may also have an important role in the enhanced stability.

Conclusions

Complex **2**, an iron–nitroxyl complex derived from a porphyrin, is obtained quantitatively by one-electron reduction of complex **1**, and unlike [Fe(TPP)NO]⁻ and [Fe(OEP)NO]⁻, it can be isolated and is stable in CH₂Cl₂ indefinitely as long as oxygen is excluded. This enhanced stability with respect to

[Fe(TPP)NO]⁻ and [Fe(OEP)NO]⁻, the only previously reported iron–nitroxyl porphyrin complexes, is achieved thanks to the electron-withdrawing groups present in the porphyrin ring, as can be concluded from the highly positively shifted reduction potentials in the voltammogram of **1**. Importantly, despite the considerable effect of the withdrawing groups in the stabilization of **2** toward oxidation, there is no dramatic change in its electronic structure, compared to other {Fe(Porph)NO}⁸, which makes **2** a good candidate for a heme {FeNO}⁸ model.

According to FTIR, UV–vis, ¹⁵N NMR, and DFT results, we could assign the electronic structure of **2** as intermediate between Fe^{II}NO⁻ and Fe^INO. As far as we know, this is the first assignment of the electronic structure of the heme {FeNO}⁸ from both experimental and computational data. The ¹⁵N NMR result is irrefutable evidence of an {MNO}⁸ complex and has not been previously reported for an Fe^{II}NO⁻ system. Comparison of **2** with the non-heme {FeNO}⁸ complex Fe(NO)(cyclam-ac),⁷ shows a big difference in their electronic structures. The non-heme system fits well the limiting description of Fe^{II}NO⁻; the most sensitive parameters to the degree of reduction of the NO ligand are the N–O distance and the ν_{NO} stretching frequency.

In conclusion, we have succeeded in stabilizing the heme {FeNO}⁸ by controlling its reduction potential with a perhalogenated iron II porphyrinate. We expect to further characterize complex **2**, studying its reactivity toward other ligands and electrophiles. Since there is a second, well reversible reduction wave in the voltammogram of **1**, special emphasis will be placed on the characterization of the second reduction product of **1**.

Acknowledgment. We thank UBA, CONICET, and ANPCyT for financial support, and Prof. D. Estrin for helpful discussions on DFT.

Supporting Information Available: Experimental details for the synthesis of Fe^{III}(TFPPBr₈)Cl, complete cyclic voltammogram of **1**, FTIR and UV–vis spectra of **1**, complete FTIR spectra of Fe^{III}(TFPPBr₈)Cl, FTIR spectra of labeled **2** in CH₂Cl₂, UV–vis and FTIR spectra of the reaction of **2** with ferrocenium hexafluorophosphate and triflic acid, UV–vis spectra of the reaction of **2** with acetic acid, complete ¹H and ¹⁵N NMR spectra of **2**, Cartesian coordinates from optimizations and frontier orbitals for **2** and Fe(Porphine)NO⁻ and complete reference 18. This material is available free of charge via the Internet at <http://pubs.acs.org>.

JA905062W